ASEC 2022

MDPI

Type of the Paper (Article, Review, Communication, etc.)

Effects of addition of copper chloride and potassium iodide to methylammonium-based perovskite solar cells

Ayu Enomoto [1], Atsushi Suzuki [1,*], Takeo Oku [1], Masanobu Okita [2], Sakiko Fukunishi [2], Tomoharu Tachikawa [2], and Tomoya Hasegawa [2]

[1] Department of Materials Science, The University of Shiga Prefecture, 2500 Hassaka, Hikone, Shiga 522-8533, Japan; oe21aenomoto@ec.usp.ac.jp (A.E.); oku@mat.usp.ac.jp (T.O.)
[2] Osaka Gas Chemicals Co., Ltd., 5-11-61 Torishima, Konohana-ku, Osaka 554-0051, Japan; okita@ogc.co.jp (M.O.); fukunishi@ogc.co.jp (S.F.); t-tachikawa@ogc.co.jp (T.T.); hasegawa_tomoya@ogc.co.jp (T.H.)
* Correspondence: suzuki@mat.usp.ac.jp (A.S.); Tel.: +81-749-28-8369

Abstract: Organic-inorganic hybrid perovskite solar cells have advantage to apply commercial products of photovoltaic devices with high conversion efficiency, easy fabrication process and low cost. The perovskite solar cells have the photovoltaic performance with reduced durability due to the volatility of organic cations and toxic lead in the perovskite crystal as active layer. The purpose of this research is to investigate effect of additives such as cupper chloride and potassium iodide into the perovskite crystal on the photovoltaic properties and electronic structure. The distribution of 3d orbital of cupper ion conjugated with 5p orbital of iodine ion at the valence band, and 6p orbital of lead ion at the conduction band, influencing the charge generation and transfer, and carrier mobility with narrowing band gap. The addition of potassium iodide caused to delocalize the charge distribution near cupper, iodide and lead ions, which promoted the charge generation and carrier diffusion, yielding increase of short circuit current density related to conversion efficiency.

Keywords: perovskite; solar cell; photovoltaic device; copper; methylammonium; potassium; polysilane; decaphenylcyclopentasilane

Citation: Lastname, F.; Lastname, F.; Lastname, F. Title. *Appl. Sci.* **2022**, *12*, x. https://doi.org/10.3390/xxxxx

Academic Editor: Firstname Lastname

Received: date
Accepted: date
Published: date

Publisher's Note: MDPI stays neutral with regard to jurisdictional claims in published maps and institutional affiliations.

1. Introduction

Lead halide perovskite semiconductors attracted attention as the active layer of electroluminescence in the 1990s [1]. After the first application of a $CH_3NH_3PbI_3$ compound to solar cells [2], the lead halide perovskites have been actively researched worldwide [3-7]. Since $CH_3NH_3PbI_3$ perovskite solar cells have high sensitivity to visible light and easy production process, it is expected next-generation solar cells. However, toxicity problems in including Pb perovskite solar cells have impeded their wholescale commercial application. Moreover, long-term instability caused by decomposition of perovskite crystal still hasn't reached a resolution. Contamination of soil and water by Pb^{2+} ions is permanent. When organisms take in Pb, it is not eliminated from the body and causes serious adverse effects. It enters the human body and causes dysfunction in the nervous, digestive, and blood systems. It is mandatory to provide safe and environmentally friendly products. From previous studies, less toxic ions such as Sn^{2+}, Ge^{2+}, Co^{2+}, and Cu^{2+} are expected to be alternative elements [8-12]. Among them, the environmentally friendly transition metal Cu^{2+} has been examined as a candidate for Pb^{2+} replacement, but there are few reported cases [13-15]. In addition, the durability of perovskite solar cell is caused mainly by the decomposition of the perovskite crystals due to methylammonium (MA) desorption. To

solve problems, attempts to introduce additives into the perovskite layer to improve the electronic properties have been studied [16-27]. Previous studies have reported that substitution of potassium (K) can inhibit MA desorption resulting in improved performance and long-term stability [28-33]. The aim of this work is to fabricate and characterize the perovskite solar cell doped with cupper chloride and potassium iodide. The photovoltaic properties, morphologies, and crystal structure were investigated by substitution of Cu^{2+} and K^{+} ions. The stability of the performance was measured. In addition, first-principles calculations were performed as compared with experimental results.

2. Materials and Methods

The present perovskite solar cells were prepared according to the literatures [34-38]. For preparing the perovskite compound, a mixture of CH_3NH_3I (MAI, Tokyo Chemical Industry, 2.4 M), $PbCl_2$ (0.8 M, Sigma-Aldrich), copper chloride ($CuCl_2$, Sigma Aldrich), potassium iodide (KI, Wako Pure Chemical Corporation) with the desired molar ratio in *N*,*N*-dimethylformamide (DMF, NacalaiTesque, Kyoto, Japan, 0.5 mL) was stirred at 60°C for 24 h. As standard recipe, the mole of MAI and $PbCl_2$ in DMF was adjusted to be 2.4 M (190.8 mg) and 0.8 M (111.2 mg). In the doped case of 2% $CuCl_2$, the mole of MAI, $PbCl_2$ and $CuCl_2$ was adjusted to be 2.4 M (190.8 mg), 0.78 M (109.0 mg) and 0.02 M (1.07 mg). In the doped case of 2% $CuCl_2$ and 2% KI, the mole of MAI, $PbCl_2$, KI and $CuCl_2$ was adjusted to be 2.35 M (186.9 mg), 0.78 M (109 mg), 0.01 M (0.93 mg) and 0.02 M (1.07 mg). The perovskite solutions were spin-coated on TiO_2 with air flow at three times. A solution of decaphenylcyclopentasilane (DPPS, Osaka Gas Chemical, OGSOL SI-30-15, 10 mg) was prepared in chlorobenzene (0.5 mL) and dropped onto the perovskite layer during the last stage of the spin-coating process. DPPS was used as a hole-transporting material with protecting of the cell from moisture and oxygen. Annealing process was performed at 200°C. All procedures were performed in air atmosphere. A gold (Au) electrode was deposited to serve as the top electrode. The structure of the solar cells is denoted as FTO/TiO_2/perovskite/DPPS/spiro-OMeTAD/Au. The prepared cells were stored at temperature of 22°C and humidity below 30%.

The electronic structures of the Cu-, and K-doped perovskite crystal were single-point calculated by ab initio quantum calculation [39-45] based on the restricted Hartree–Fock method and hybrid density functional theory (DFT) using restricted B3LYP with LANL2MB as the basis set (Gaussian 09). The $MAPbI_3$ perovskite crystals with supercells of 2 × 2 × 2 as cluster model were formed on the basis of the experimental results using X-ray diffraction data.

3. Results and discussion

3.1. First-principles calculation

Electron density distributions at the highest occupied molecular orbital (HOMO) and lowest unoccupied molecular orbital (LUMO), electrostatic potential (ESP) and partial charge of MAPb(Cu)I_3 and MA(K)Pb(Cu)I_3 perovskite cubic crystals with 2 × 2 × 2 supercells are shown in Fig. 1(a) and (b), respectively. The electron density distributions of the MAPb(Cu)I_3 perovskite demonstrated that the 6p orbitals of the Pb atom dominated at the LUMO. The 3d orbitals of Cu^{2+} ion and the 5p orbitals of the I^{-} ion were delocalized at HOMO. The charge transfer between 3d orbitals of Cu^{2+} ion and 5p orbital of the I^{-} ion would promote the carrier generation and carrier diffusion.

The electron density distributions of the MA(K)Pb(Cu)I_3 perovskite are shown in Fig. 1b. The 6p orbitals of the Pb^{2+} ion and the 4s orbitals of the Cu^{2+} ion were formed in the LUMO. The 3d orbitals of Cu^{2+} ion and the 5p orbitals of the I^{-} ion were dominated in the HOMO. Addition of K^{+} caused to form 4s orbitals of Cu^{2+} conjugated with 6p orbital of Pb

ion in the LUMO, promoting charge transfer between 4s orbital and 6p orbital in the coordination band. For the ESP and partial charge of MAPb(Cu)I_3 and MA(K)Pb(Cu)I_3 perovskite, the charges of Cu^{2+} and I^- ion were delocalized by positive charge of K^+, which would promote the carrier diffusion and increase of short circuit current density.

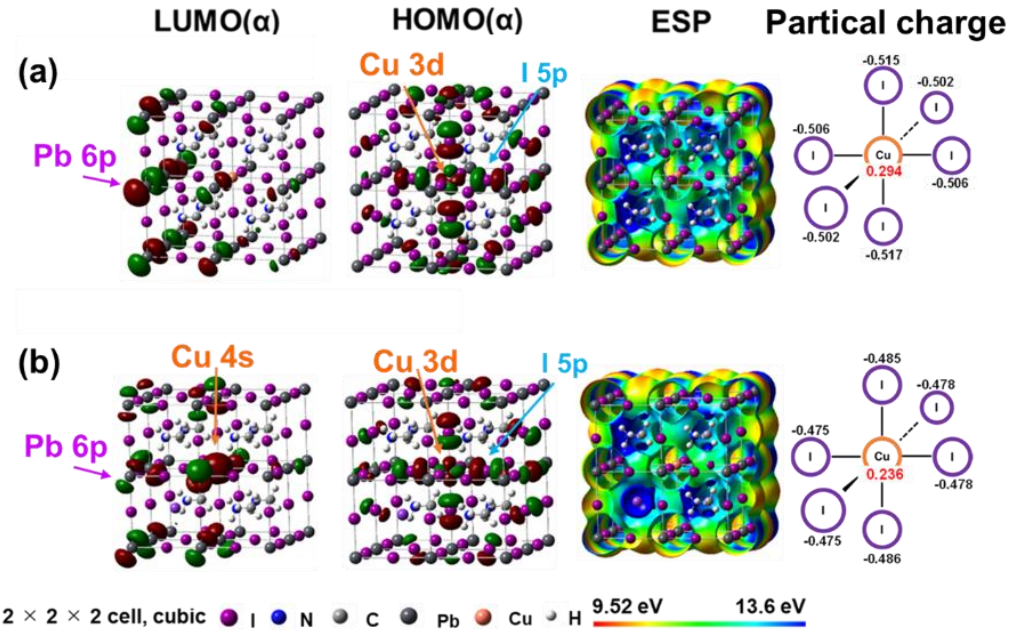

Figure 1. The electron density distributions at the highest occupied molecular orbital (HOMO) and lowest unoccupied molecular orbital (LUMO), electrostatic potential (ESP) and partial charge of (a) $MAPb_{0.963}Cu_{.0.037}I_3$ and (b) $MA_{0.875}K_{0.125}Pb_{0.963}Cu_{0.037}I_3$ perovskite cubic crystals with 2 × 2 × 2 supercells.

3.2. Device characterization

The photovoltaic parameters of open-circuit voltage (V_{OC}), short-circuit current density (J_{SC}), fill factor (FF), conversion efficiency (η) and band gap (E_g) are listed in Table 1. The conversion efficiencies of the Cu- and K-doped perovskite solar cells was obtained to be 10.59%, which were higher than that of the Cu-added solar cell. Addition of Cu^{2+} and K^+ ions supported the photovoltaic performance with increase of J_{SC} related to η, due to enhancement of the carrier transfer in the perovskite crystal.

Table 1. Photovoltaic parameters of present perovskite photovoltaic devices.

Devices	J_{SC} (mA cm^{-2})	V_{OC} (V)	FF	η (%)	η_{ave} (%)	E_g (eV)
$MAPbI_3$	21.6	0.822	0.622	11.03	9.00	1.56
$+Cu^{2+}$ 2%	18.5	0.800	0.627	9.26	8.47	1.56
$+Cu^{2+}$ 2%, K^+ 2%	21.4	0.837	0.590	10.59	8.99	1.56

4. Conclusions

Fabrication and characterization of Cu- and K-doped $MAPbI_3$ perovskite solar cell was performed. The photovoltaic properties and electronic structures were investigated. The 2% Cu- and 2% K-doped perovskite solar cell had the photovoltaic performance of conversion efficiency with increases of the *J*sc values. The charge transfer between the 3d

orbital of Cu^{2+} ion and 5p orbitals of I^- ion would influence the carrier generation and diffusion in the cubic MAPb(Cu)I_3 perovskite. Addition of K^+ into MAPb(Cu)I_3 perovskite caused to form the 3d orbital of Cu^{2+} ion in the HOMO and LUMO. The addition of K^+ caused to delocalize the 3d and 5p orbitals of Cu^{2+} and I^- ions near HOMO, and 4s and 6p orbital of Cu^{2+} and Pb^{2+} ions near LUMO with wide charge distribution, which promoted the carrier generation and charge transfer, yielding increase of J_{SC} related to η.

Author Contributions: Conceptualization, A.E.; methodology, A.E., A.S. and T.O.; formal analysis, A.E., A.S. and T.O; investigation, A.E.; resources, A.E., A.S. and T.O; data curation, A.E., A.S. and T.O; writing—original draft preparation, A.E., A.S. and T.O; project administration, A.E., A.S. and T.O; funding acquisition, A.E., A.S. and T.O.

Funding: This research was supported by JSPS KAKENHI Grant Number JP 21K05261.

Institutional Review Board Statement: Not applicable.

Informed Consent Statement: Not applicable.

Data Availability Statement: Data is contained within the article.

Conflicts of Interest: The authors declare no conflict of interest.

References

1. Chondroudis, K.; Mitzi, D.B. Electroluminescence from an organic–inorganic perovskite incorporating a quaterthiophene dye within lead halide perovskite layers. *Chem. Mater.* **1999**, *11*, 3028, https:// doi.org/10.1021/CM990561T.
2. Kojima, A.; Teshima, K.; Shirai, Y.; Miyasaka, T. Organometal halide perovskites as visible-light sensitizers for photovoltaic cells. *J. Am. Chem. Soc.* **2009**, *131*, 6050, https://doi.org/10.1021/ja809598r.
3. Kovalenko, M.V.; Protesescu, L.; Bodnarchuk, M.I. Properties and potential optoelectronic applications of lead halide perovskite nanocrystals. *Science* **2017**, *358*, 745–750, https://doi.org/10.1126/science.aam7093.
4. Wang, D.; Wright, M.; Elumalai, N.K.; Uddin, A. Stability of perovskite solar cells. *Sol. Energy Mater Sol. Cells*. **2016,** 147, 255.
5. Chen, S.; Dai, X.; Xu, S.; Jiao, H.; Zhao, L.; Huang, J. Stabilizing perovskite-substrate interfaces for high-performance perovskite modules. *Science.* **2021**, *373*, 902, https://doi.org/10.1126/science.abi6323.
6. Zou, Y.; Teng, P.; Xu, W.; Zheng, G.; Lin, W.; Yin, J.; Kobera, L.; Abbrent, S.; Li, X.; Steele, J.A.; et al. Manipulating crystallization dynamics through chelating molecules for bright perovskite emitters. *Nat. Commun.* **2021**, *12*, 1–10, https://doi.org/10.1038/s41467-021-25092-7.
7. Wang, Y.; Mahmoudi, T.; Hahn, Y. Highly stable and efficient perovskite solar cells based on FAMA-perovskite-Cu:NiO composites with 20.7% efficiency and 80.5% fill factor. *Adv. Energy Mater.* **2020**, *10*, 27, https://doi.org/10.1002/aenm.202000967.
8. Noel, N.K.; Stranks, S.D.; Abate, A.; Wehrenfennig, C.; Guarnera S.; et al. Lead-free organic-inorganic tin halide perovskites for photovoltaic applications. *Energy Environ. Sci.* **2014**, *9*, 3061–3068. https://doi.org/10.1039/c4ee01076k.
9. Krishnamoorthy, T.; Ding, H.; Yan, C.; Leong, W.L.; Baikie, T.; et al. Lead-free germanium iodide perovskite materials for photovoltaic applications. *J. Mater. Chem.* A **2015**, *47*, 23829–23832. https://doi.org/10.1039/c5ta05741h.
10. Li, Y.; Zhou, Z.; Tewari, N.; Ng, M.; Geng, P.; Chen, D.; Ko, P.K.; Qammar, M.; Guo, L.; Halpert, J.E. Progress in copper metal halides for optoelectronic applications. *Mater. Chem. Front.* **2021**, *5*, 4796–4820, https://doi.org/10.1039/D1QM00288K.
11. Li, M.; Wang, Z.K.; Zhuo, M.P.; Hu, Y.; Hu, K.H.; Ye, Q.Q.; Jain, S.M.; Yang, Y.G.; Gao, X.Y.; Liao, L.S. Pb-Sn-Cu ternary organometallic halide perovskite solar cells. *Adv. Mater.* **2018**, *30*, e1800258, https://doi.org/10.1002/adma.201800258.
12. Suzuki, A.; Oe, M.; Oku, T. Fabrication and characterization of Ni-, Co-, and Rb-incorporated $CH_3NH_3PbI_3$ perovskite solar cells. *J. Electron. Mater.* **2021**, *50*, 1980–1995, https://doi.org/10.1007/s11664-021-08759-1.
13. Ueoka, N.; Oku, T.; Suzuki, A. Effects of doping with Na, K, Rb, and formamidinium cations on $(CH_3NH_3)_{0.99}Rb_{0.01}Pb_{0.99}Cu_{0.01}I_{3-x}(Cl,Br)_x$ perovskite photovoltaic cells. *AIP Adv.* **2020**, *10*, 125023, https://doi.org/10.1063/5.0029162.
14. Ge, X.; Qu, X.; He, L.; Sun, Y.; Guan, X.; Pang, Z.; Wang, C.; Yang, L.; Wang, F.; Rosei, F. 3D low toxicity Cu–Pb binary perovskite films and their photoluminescent/photovoltaic performance. *J. Mater. Chem.* A **2019**, 7, 27225–27235, https://doi.org/10.1039/C9TA12736D.
15. Ueoka, N.; Oku, T. Effects of co-addition of sodium chloride and copper (II) bromide to mixed-cation mixed-halide perovskite photovoltaic devices. *ACS Appl. Energy Mater.* **2020**, *3*, 7272–7283, https://doi.org/10.1021/acsaem.0c00182.
16. Oku, T. Crystal structures of perovskite halide compounds used for solar cells. *Rev. Adv. Mater. Sci.* **2020**, *59*, 264–305, https://doi.org/10.1515/rams-2020-0015.
17. Wu, C.; Chen, K.; Guo, D.Y.; Wang, S.L.; Li, P.G. Cations substitution tuning phase stability in hybrid perovskite single crystals by strain relaxation. *RSC Adv.* **2018**, *8*, 2900–2905, https://doi.org/10.1039/c7ra12521f.

18. Tavakoli, M.M.; Zakeeruddin, S.M.; Grätzel, M.; Fan, Z. Large-grain tin-rich perovskite films for efficient solar cells via metal alloying technique. *Adv. Mater.* **2018**, *30*, 11, https://doi.org/10.1002/adma.201705998.
19. Oku, T.; Ohishi, Y.; Suzuki, A. Effects of antimony addition to perovskite-type $CH_3NH_3PbI_3$ photovoltaic devices. *Chem. Lett.* **2016**, *45*, 134, https://doi.org/10.1246/cl.171214.
20. Li, M.; Wang, Z.K.; Zhuo, M.P.; Hu, Y.; Hu, K.H.; Ye, Q.Q.; Jain, S.M.; Yang, Y.G.; Gao, X.Y.; Liao, L.S. Pb-Sn-Cu ternary organometallic halide perovskite solar cells. *Adv. Mater.* **2018**, *30*, e1800258, https://doi.org/10.1002/adma.201800258.
21. Ge, X.; Qu, X.; He, L.; Sun, Y.; Guan, X.; Pang, Z.; Wang, C.; Yang, L.; Wang, F.; Rosei, F. 3D low toxicity Cu–Pb binary perovskite films and their photoluminescent/photovoltaic performance. *J. Mater. Chem. A* **2019**, *7*, 27225–27235, https://doi.org/10.1039/c9ta12736d.
22. Elseman, A.M.; Shalan, A.E.; Sajid, S.; Rashad, M.M.; Hassan, A.M.; Li, M. Copper-substituted lead perovskite materials constructed with different halides for working $(CH_3NH_3)_2CuX_4$-based perovskite solar cells from experimental and theoretical view. *ACS Appl. Mater. Interfaces* **2018**, *10*, 11699–11707, https://doi.org/10.1021/acsami.8b00495.
23. Tanaka, H.; Ohishi, Y.; Oku, T. Fabrication and characterization of the copper bromides-added $CH_3NH_3PbI_{3-x}Cl_x$ perovskite solar cells. *Synth. Met.* **2018**, *244*, 128, https://doi.org/10.1016/j.synthmet.2018.07.008Get rights and content.
24. Ueoka, N.; Oku, T.; Suzuki, A. Additive effects of alkali metals on Cu-modified $CH_3NH_3PbI_{3-\delta}Cl_\delta$ photovoltaic devices, *RSC Adv.* **2019**, *9*, 24231, https://doi.org/10.1039/C9RA03068A.
25. Li, Y.; Zhou, Z.; Tewari, N.; Ng, M.; Geng, P.; Chen, D.; Ko, P.K.; Qammar, M.; Guo, L.; Halpert, J.E. Progress in copper metal halides for optoelectronic applications. *Mater. Chem. Front.* **2021**, *5*, 4796–4820, https://doi.org/10.1039/d1qm00288k.
26. Karthick, S.; Hawashin, H.; Parou, N.; Vedraine, S.; Velumani, S.; Boucle, J. Copper and bismuth incorporated mixed cation perovskite solar cells by one-step solution process. *Sol. Energy*, **2021,** *218*, 226, https://doi.org/10.1016/j.solener.2021.02.053.
27. Wang, K.-L.; Wang, R.; Wang, Z.K.; Li, M.; Zhang, Y.; Ma, H.; Liao, L.-S.; Yang, Y. Tailored phase transformation of $CsPbI_2Br$ films by copper(II) bromide for high-performance all-inorganic perovskite solar cells. *Nano Lett.* **2019**, *19*, 5176–5184, https://doi.org/10.1021/acs.nanolett.9b01553.
28. Tang, Z.; Bessho, T.; Awai, F.; Kinoshita, T.; Maitani, M.; Jono, R.; Murakami, T.N.; Wang, H.; Kubo, T.; Uchida, S.; et al. Hysteresis-free perovskite solar cells made of potassium-doped organometal halide perovskite. *Sci. Rep.* **2017,** *7*, 12183, https://doi.org/10.1038/s41598-017-12436-x.
29. Alanazi, T.I.; Game, O.S.; Smith, J.A.; Kilbride, R.C.; Greenland, C.; Jayaprakash, R.; Georgiou, K.; Terrill, N.J.; Lidzey, D.G. Potassium iodide reduces the stability of triple-cation perovskite solar cells. *RSC Adv.* **2020**, *10*, 40341–40350, https://doi.org/10.1039/D0RA07107B.
30. Kandori, S.; Oku, T.; Nishi, K.; Kishimoto, T.; Ueoka, N.; Suzuki, A. Fabrication and characterization of potassium- and formamidinium-added perovskite solar cells. *J. Ceram. Soc. Jpn.* **2020,** *128*, 805–811, https://doi.org/10.2109/jcersj2.20090.1.
31. Jiang, J.; Xu, J.; Walter, H.; Kazi, A.; Wang, D.; Wangila, G.; Mortazavi, M.; Yan, C.; Jiang, Q. The doping of alkali metal for halide perovskites. *ES Mater. Manuf.* **2020**, 7, 25–33, https://doi.org/10.30919/esmm5f705.
32. Oku, T.; Zushi, M.; Imanishi, Y.; Suzuki, A.; Suzuki, K. Microstructures and photovoltaic properties of perovskite-type $CH_3NH_3PbI_3$ compounds. *Appl. Phys. Express* **2014**, *7*, 121601, https://doi.org/10.7567/apex.7.121601.
33. Machiba, H.; Oku, T. Kishimoto, T.; Ueoka, N.; Suzuki, A. Fabrication and evaluation of K-doped $MA_{0.8}FA_{0.1}K_{0.1}PbI_3$(Cl) perovskite solar cells. *Chem. Phys. Lett.* **2019**, *730*, 117, https://doi.org/10.1016/j.cplett.2019.05.050.
34. Oku, T.; Ohishi, Y.; Ueoka, N. Highly (100)-oriented $CH_3NH_3PbI_3$(Cl) perovskite solar cells prepared with NH_4Cl using an air blow method. *RSC Adv.* **2018**, *8*, 10389–10395, https://doi.org/10.1039/c7ra13582c.
35. Oku, T.; Kandori, S.; Taguchi, M.; Suzuki, A.; Okita, M.; Minami, S.; Fukunishi, S.; Tachikawa, T. Polysilane-inserted methylammonium lead iodide perovskite solar cells doped with formamidinium and potassium. *Energies* **2020**, *13*, 4776, https://doi.org/10.3390/en13184776.
36. Taguchi, M.; Suzuki, A.; Oku, T.; Ueoka, N.; Minami, S.; Okita, M. Effects of annealing temperature on decaphenylcyclopentasilane-inserted $CH_3NH_3PbI_3$ perovskite solar cells. *Chem. Phys. Lett.* **2019**, *737*, 136822, https://doi.org/10.1016/j.cplett.2019.136822.
37. Oku, T.; Ueoka, N.; Suzuki, K.; Suzuki, A.; Yamada, M.; Sakamoto, H.; Minami, S.; Fukunishi, S.; Kohno, K.; Miyauchi S.; Fabrication and characterization of perovskite photovoltaic devices with TiO_2 nanoparticle layers. *AIP Conf. Proc.* **2017**, *1807*, 020014, https://doi.org/10.1063/1.4974796.
38. Oku, T.; Taguchi, M.; Suzuki, A.; Kitagawa, K.; Asakawa, Y.; Yoshida, S.; Okita, M.; Minami, S.; Fukunishi, S.; Tachikawa, T. Effects of polysilane addition to chlorobenzene and high temperature annealing on $CH_3NH_3PbI_3$ perovskite photovoltaic devices. *Coatings* **2021**, *11*, 665, https://doi.org/10.3390/coatings11060665.
39. Suzuki, A.; Oku, T. First-principles calculation study of electronic structures of alkali metals (Li, K, Na and Rb)-incorporated formamidinium lead halide perovskite compounds. *Appl. Surf. Sci.* **2019**, *483*, 912–921, https://doi.org/10.1016/j.apsusc.2019.04.049.
40. Suzuki, A.; Miyamoto, Y.; Oku, T. Electronic structures, spectroscopic properties, and thermodynamic characterization of sodium- or potassium- incorporated $CH_3NH_3PbI_3$ by first principles calculation. *J. Mater. Sci.* **2020**, *55*, 9728, https://doi.org/10.1007/s10853-020-04511-y.

41. Suzuki, A.; Oku, T. Effects of mixed-valence states of Eu-doped $FAPbI_3$ perovskite crystals studied by first-principles calculation. *Mater. Adv.* **2021**, *2*, 2609–2616, https://doi.org/10.1039/d0ma00994f.
42. Ono, I.; Oku, T.; Suzuki, A.; Asakawa, Y.; Terada, S.; Okita, M.; Fukunishi, S.; Tachikawa, T. Fabrication and characterization of $CH_3NH_3PbI_3$ solar cells with added guanidinium and inserted with decaphenylpentasilane. *Jpn. J. Appl. Phys.* **2022**, *61*, SB1024, https://doi.org/10.35848/1347-4065/ac2661.
43. Okumura, R.; Oku, T.; Suzuki, A.; Okita, M.; Fukunishi, S.; Tachikawa, T.; Hasegawa, T. Effects of adding alkali metals and organic cations to cu-based perovskite solar cells. *Appl. Sci.* **2022**, *12*, 1710, https://doi.org/10.3390/app12031710.
44. Asakawa, Y.; Oku, T.; Kido, M.; Suzuki, A.; Okumura, R.; Okita, M.; Fukunishi, S.; Tachikawa, T.; Hasegawa, T.; Fabrication and characterization of $SnCl_2$- and CuBr-added perovskite photovoltaic devices, *Technologies* **2022,** *10*, 112. https://doi.org/10.3390/technologies10060112
45. Terada, S.; Oku, T.; Suzuki, A.; Okita, M.; Fukunishi, S.; Tachikawa, T.; Hasegawa, T.; Ethylammonium bromide- and potassium-added $CH_3NH_3PbI_3$ perovskite solar cells, *Photonics*, **2022**, *9*, 791. https://doi.org/10.3390/photonics9110791